

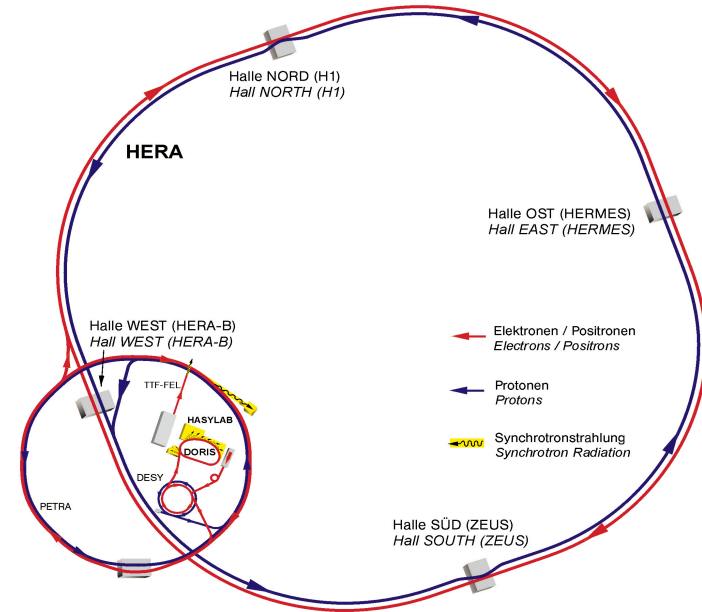
QCD and deep inelastic scattering

Alex Tapper

Slides available at:

<http://www.hep.ph.ic.ac.uk/~tapper/lecture.html>

The HERA collider



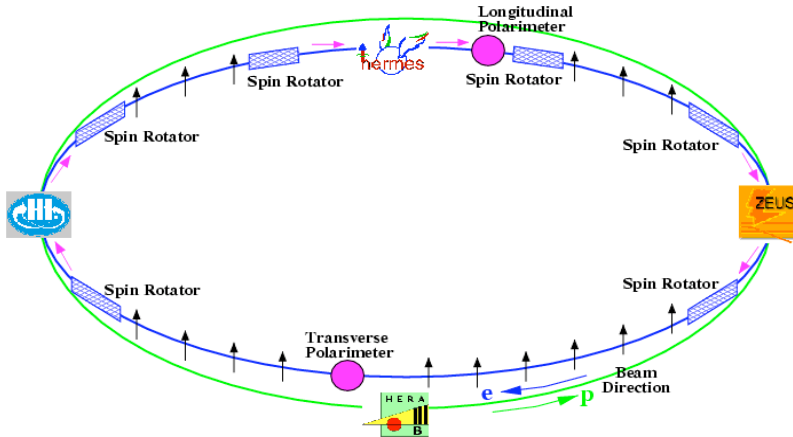
Two 6.3 km long accelerators:

Proton accelerator energy 920 GeV

Electron/positron accelerator energy
27.5 GeV

Equivalent to a 50 TeV fixed-target expt.

Lepton beam polarisation

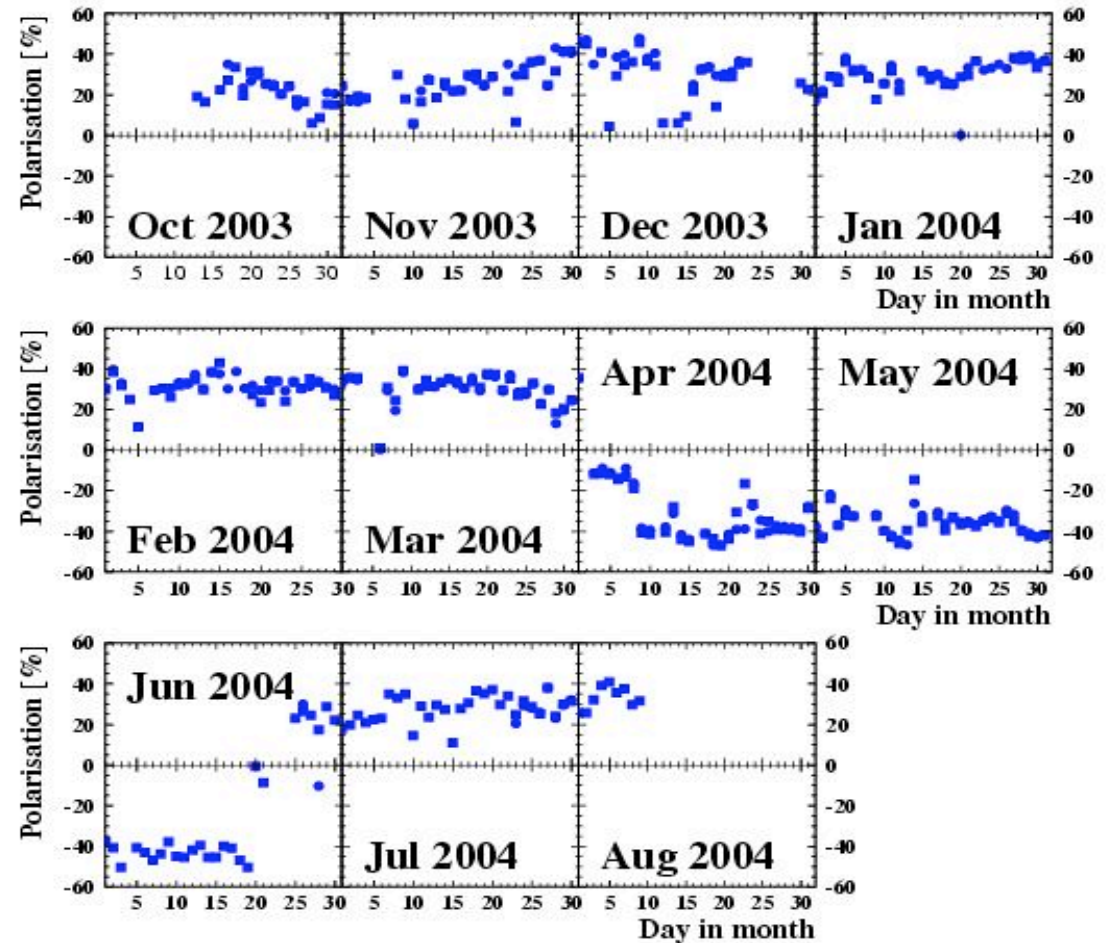


- Transverse polarisation of leptons builds up naturally through synchrotron radiation

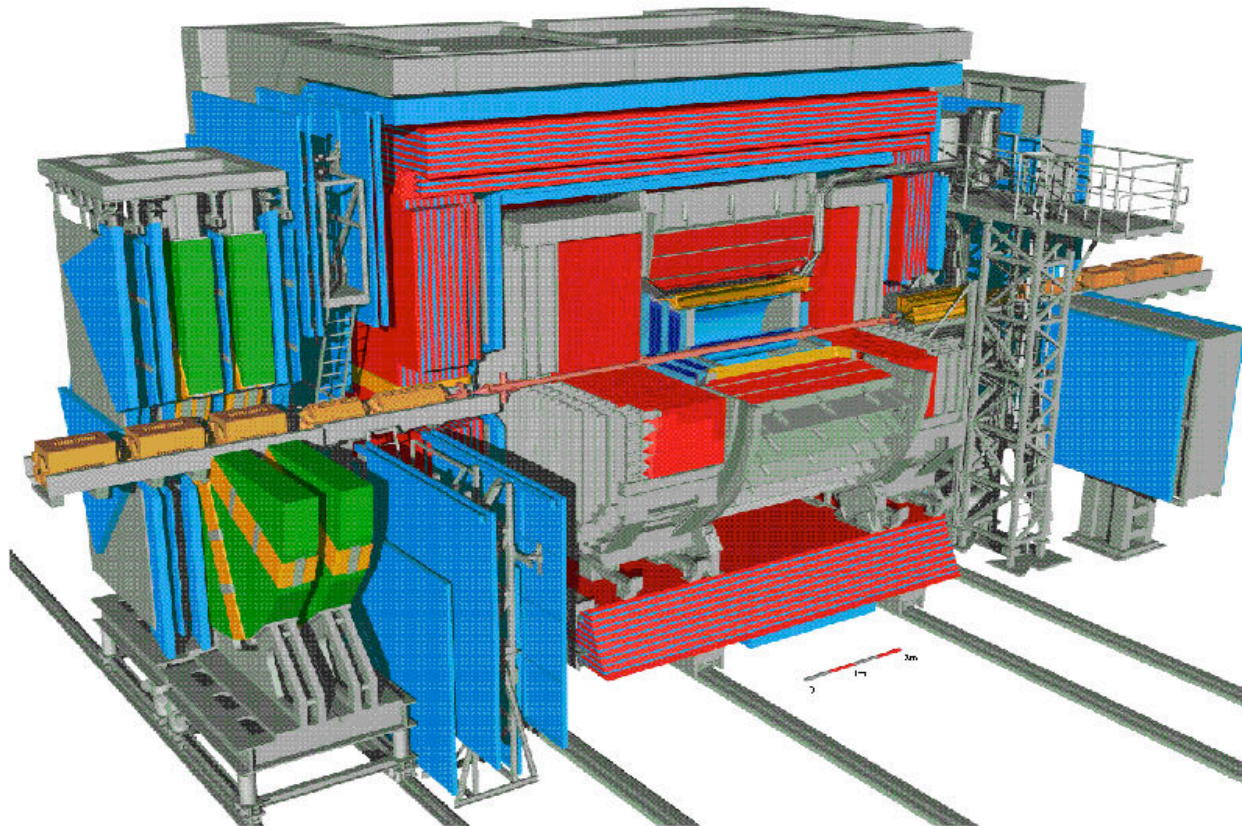
$$P_Y(t) = -P_{ST}(1 - e^{-t/\tau_{ST}})$$

- Measured by two independent Compton polarimeters
- Spin rotators convert to longitudinal polarisation
- Polarisations over 50% achieved

Average HERA polarisation



The ZEUS detector



Calorimeter

EM: $\frac{\sigma(E)}{E} = \frac{18\%}{\sqrt{E}} \oplus 1\%$

Systematic 1-2%

HAD: $\frac{\sigma(E)}{E} = \frac{35\%}{\sqrt{E}} \oplus 1\%$

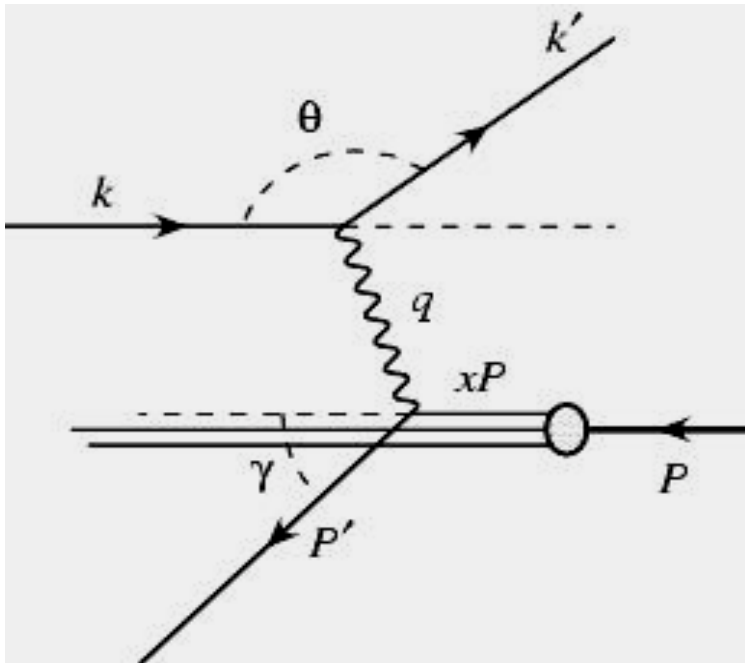
Systematic 1-2%

Tracking

Central: $15^\circ < \theta < 164^\circ$

Silicon: $7^\circ < \theta < 158^\circ$

HERA kinematics



Neutral current: exchange of γ or Z^0

Charged current: exchange of W^\pm

$$Q^2 = -q^2 = -(k - k')^2$$

$$x = \frac{Q^2}{2p \cdot q} \quad y = \frac{p \cdot q}{p \cdot k}$$

$$s = (p + k)^2 \quad Q^2 = x \cdot y \cdot s$$

- Q^2 is the probing power
- x is the Bjorken scaling variable
- y is the inelasticity

Kinematics over-constrained.

Can reconstruct event from any two of θ , γ , E_e and E_q

Neutral current DIS cross section

NC Reduced cross section: $\tilde{\sigma}_{NC}(x, Q^2)$

$$\frac{d^2 \sigma^{NC}(e^\pm p)}{dx dQ^2} = \frac{2\pi \alpha^2}{x Q^4} Y_+ \left[F_2 - \frac{y^2}{Y_+} F_L + m \frac{Y_-}{Y_+} x F_3 \right] \quad Y_\pm = 1 \pm (1-y)^2$$

Dominant contribution

Sizeable only at high y

Contribution only important at high Q^2

$$F_2 = F_2^{em} + \frac{Q^2}{Q^2 + M_Z^2} F_2^{\gamma Z} + \left[\frac{Q^2}{Q^2 + M_Z^2} \right]^2 F_2^Z \propto \sum_{q=u\dots b} (q + \bar{q})$$

$$xF_3 = \frac{Q^2}{Q^2 + M_Z^2} xF_3^{\gamma Z} + \left[\frac{Q^2}{Q^2 + M_Z^2} \right]^2 xF_3^Z \propto \sum_{q=u\dots b} (q - \bar{q})$$

Charged current DIS cross section

CC e⁺p cross section:

$$\frac{d^2\sigma^{CC}(e^+p)}{dx dQ^2} = \frac{G_F^2}{2\pi} \left(\frac{M_W^2}{M_W^2 + Q^2} \right)^2 \left[\bar{u} + \bar{c} + (1-y)^2(d+s) \right]$$

CC e⁻p cross section:

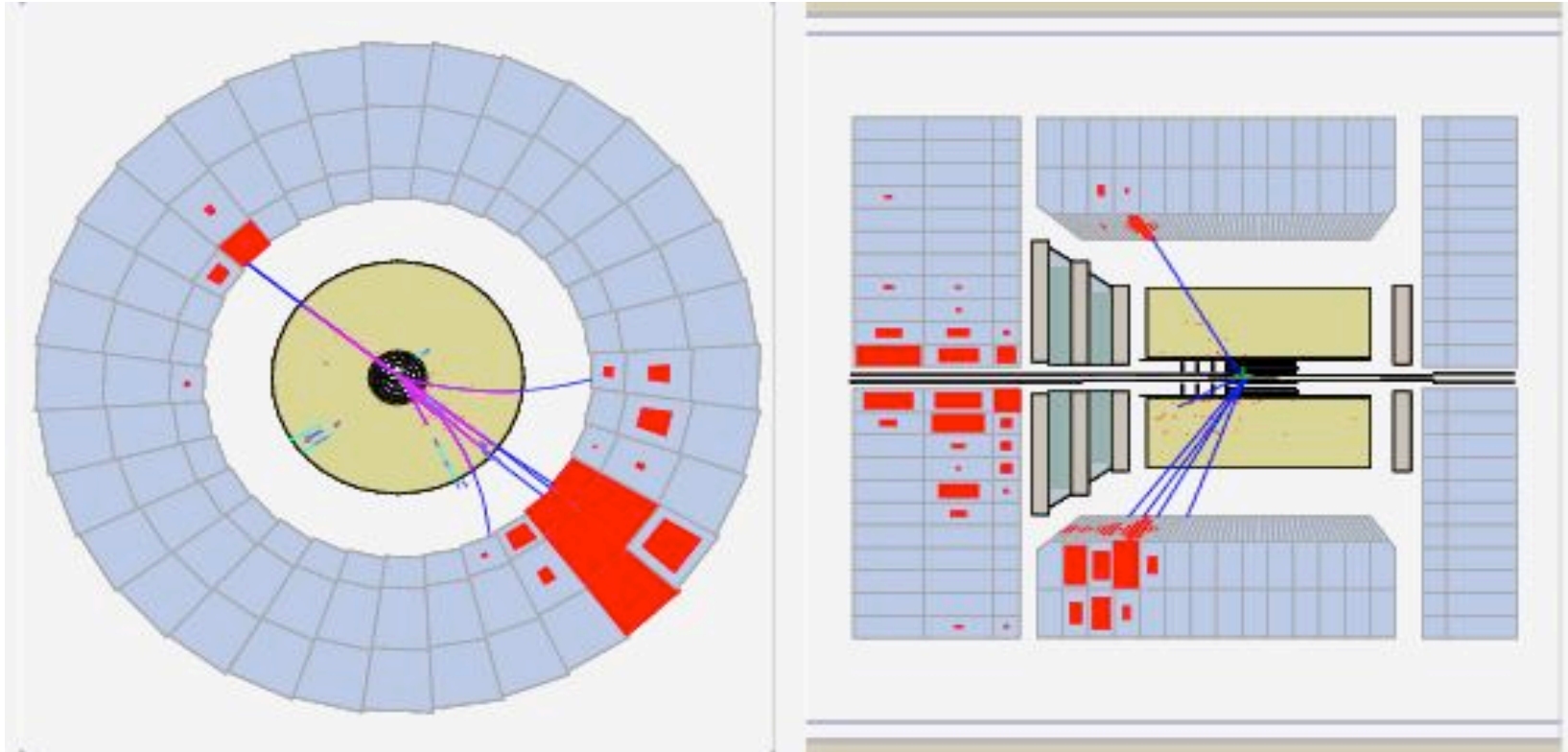
$$\frac{d^2\sigma^{CC}(e^-p)}{dx dQ^2} = \frac{G_F^2}{2\pi} \left(\frac{M_W^2}{M_W^2 + Q^2} \right)^2 \left[u + c + (1-y)^2(\bar{d} + \bar{s}) \right]$$

Electron/positron-proton collisions probe different quark content of proton

Big difference in cross section magnitude

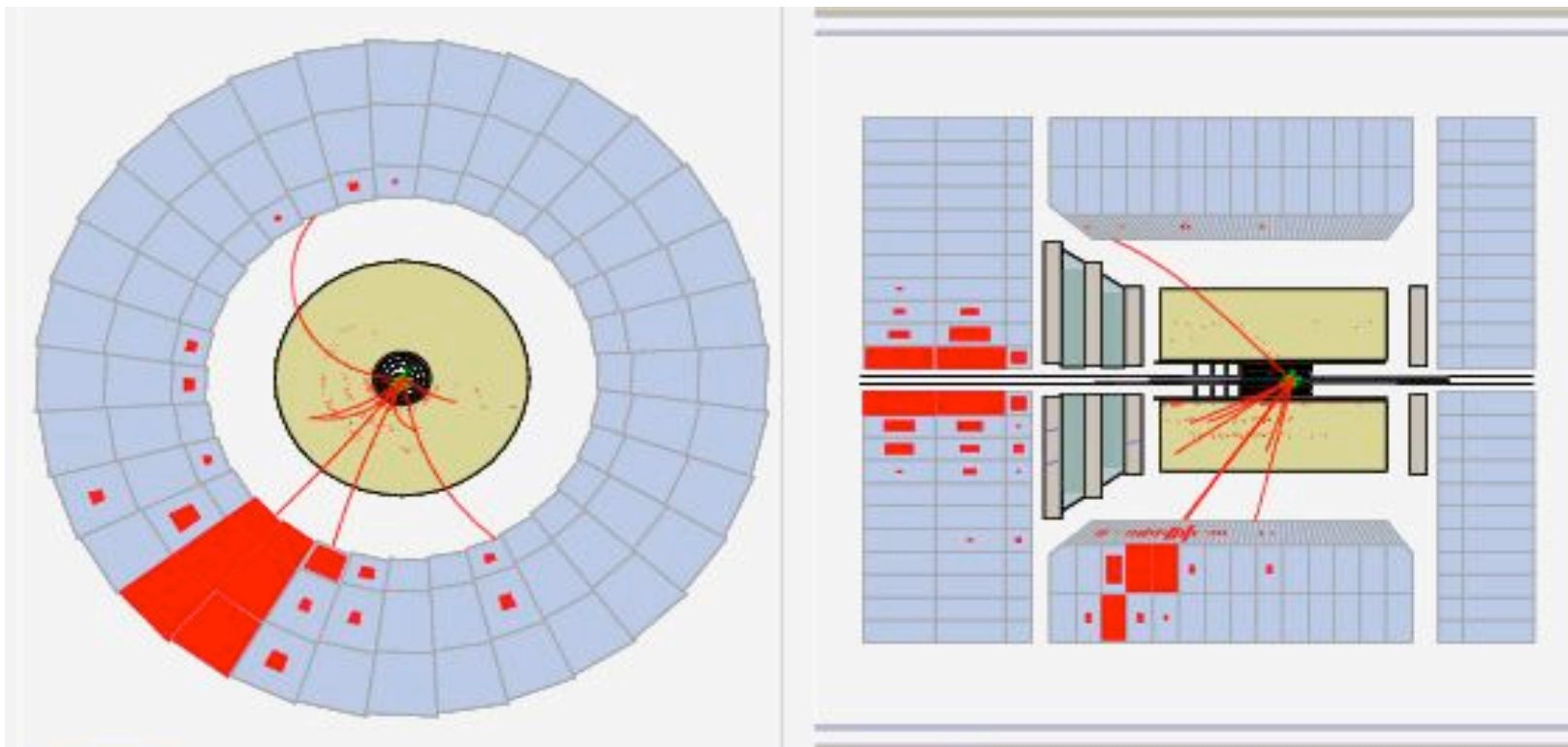
Cross sections suppressed due to large mass of W boson compared to NC DIS

NC events in the ZEUS detector



Isolated high P_T positron with hadronic jet balanced in ϕ

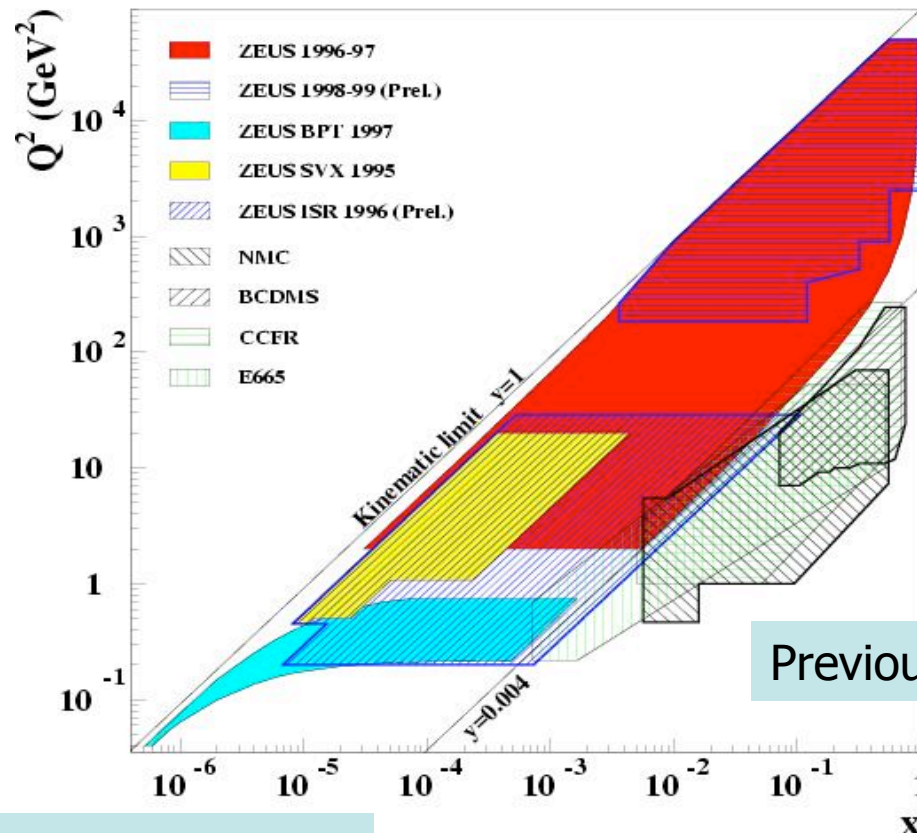
CC events in the ZEUS detector



Missing transverse momentum from the undetected neutrino

Kinematic range of HERA data

Reaching values of $Q^2 \geq 30000 \text{ GeV}^2$



Kinematic limit
defined by
 $Q^2 = sxy$

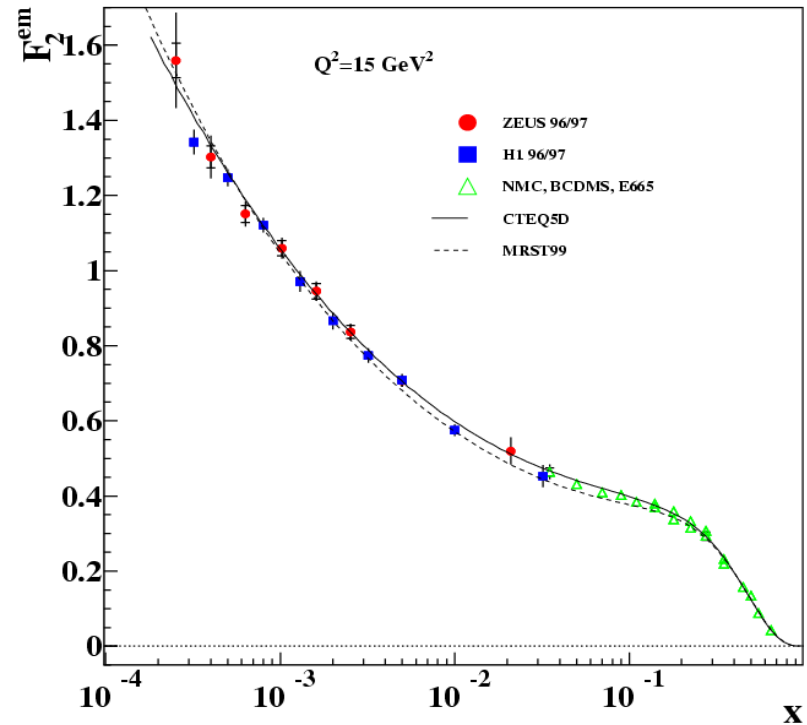
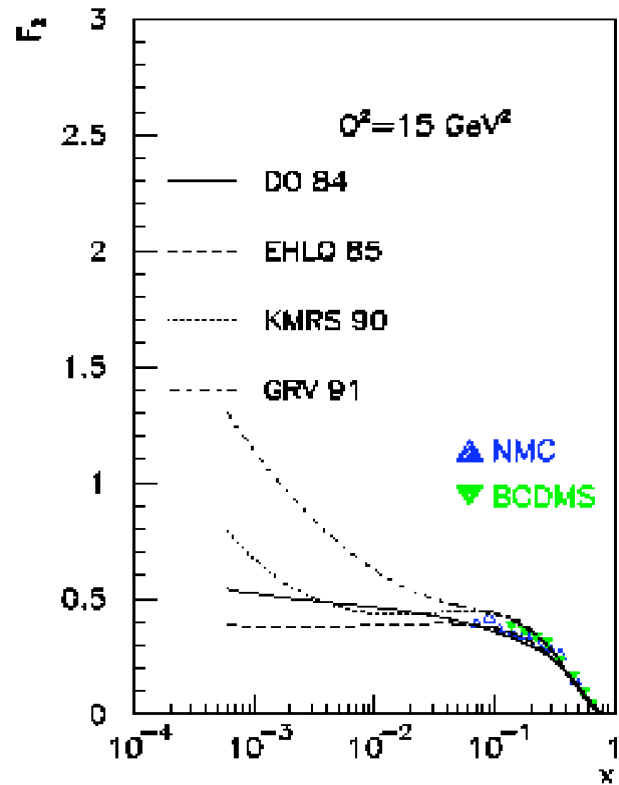
$$s_{\text{HERA}} = 1.2 \times 10^5 \text{ GeV}^2$$

Previous fixed-target experiments

Reaching values of $x < 10^{-6}$

Extension by several orders of magnitude in x and Q^2

Experimental progress

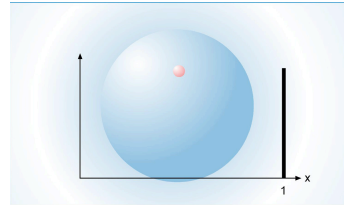


Before HERA:

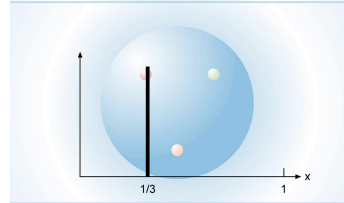
→ wide range of predictions

The shape of the proton

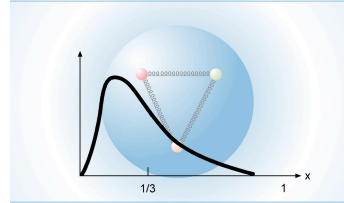
A single particle



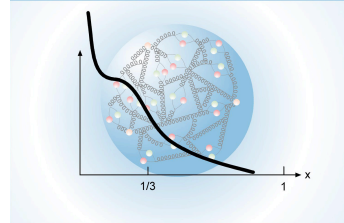
Three valence quarks



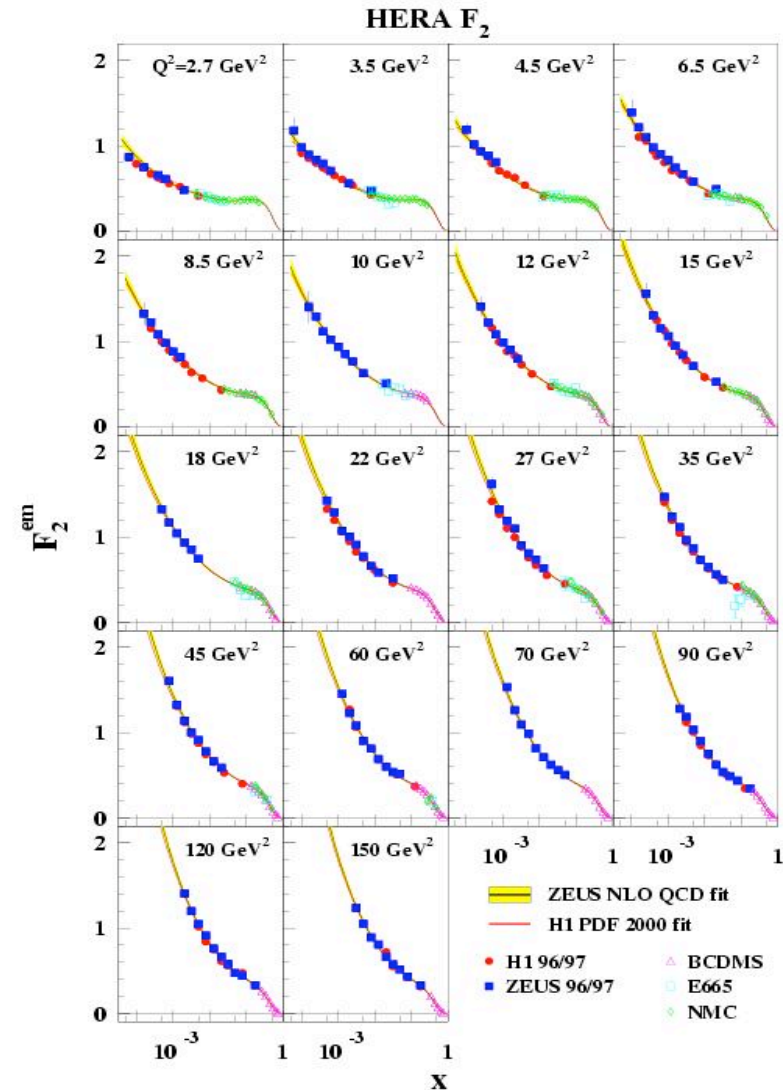
Three valence quarks with interactions



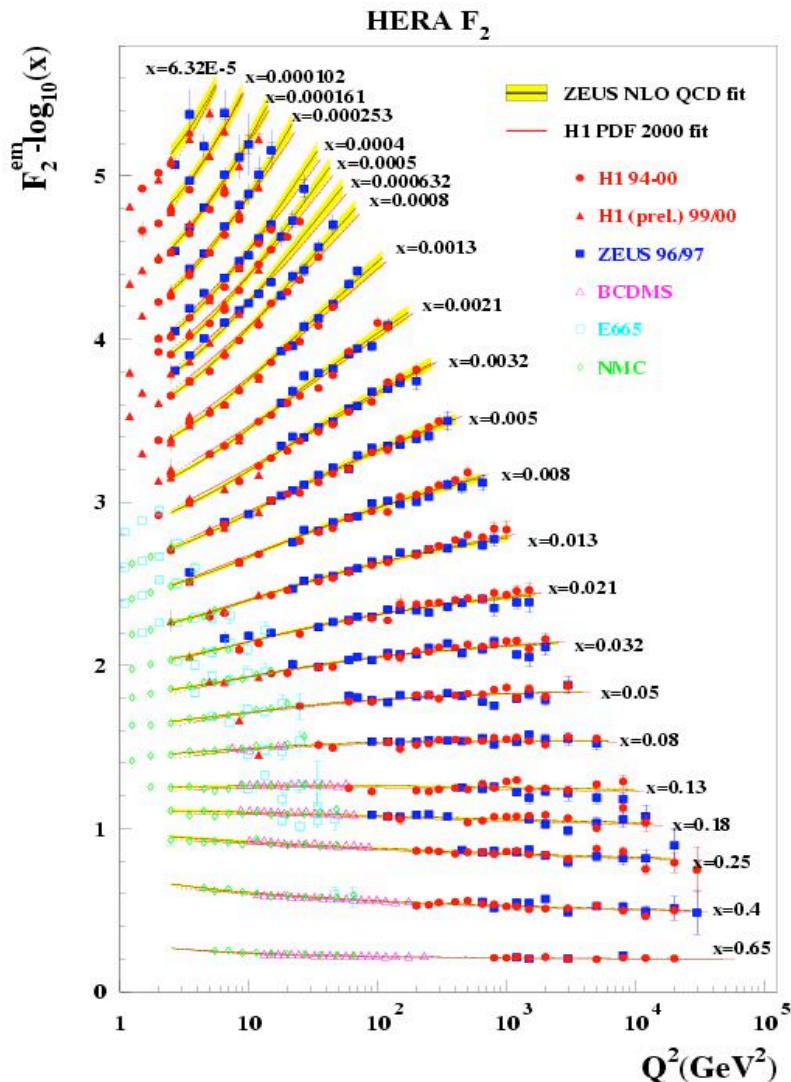
Valence and sea quarks with interactions



HERA extends proton structure measurements to low x
Rise at low x is a function of Q^2



Structure function measurements

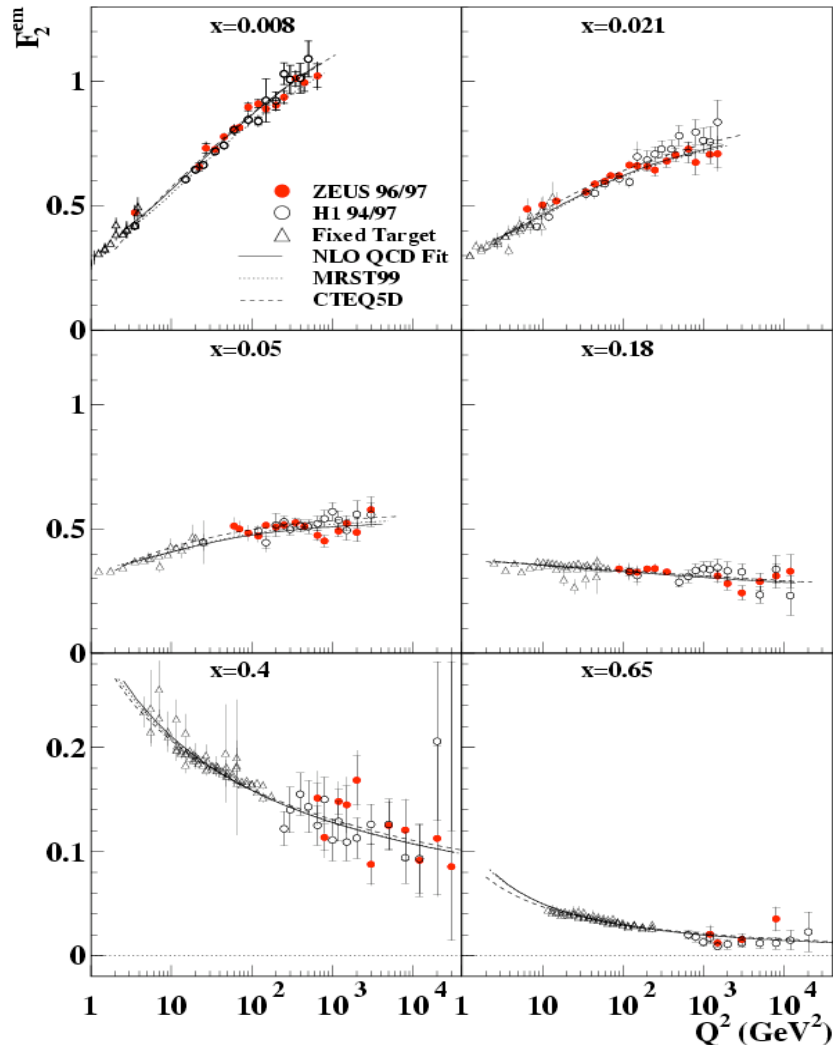


$$F_2 \propto \sum_q e_q^2 x(q + \bar{q})$$

- Impact of HERA clear
- F_2 dominates cross section
- Measured with precision of $\sim 2\text{-}3\%$
- Sensitive to sum of quarks and antiquarks
- F_2 sensitive to gluon density via QCD radiation
- Scaling violations
 - Largest at low x
 - Driven by gluon density

Scaling violations

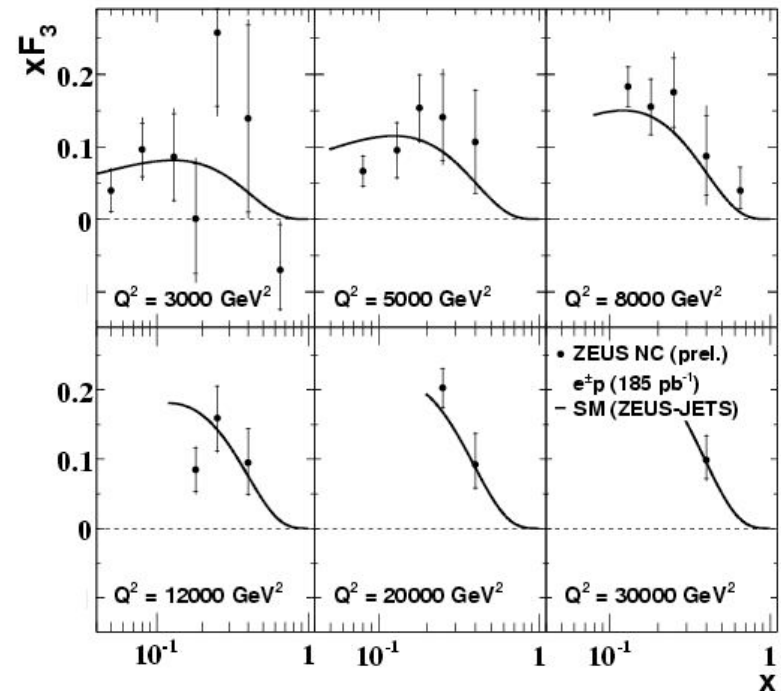
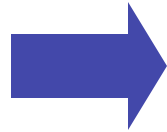
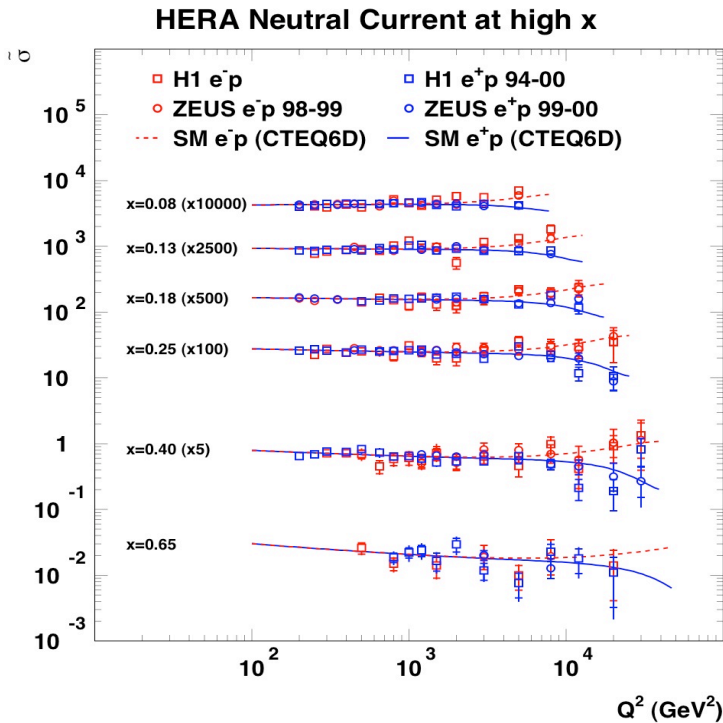
ZEUS



- Effect of QCD
 - Increase F_2 at low x
 - Decrease F_2 at high x
- Sensitivity to gluon distribution from accurate determination of scaling violations
- Quantitative test of QCD evolution

High Q^2 cross sections & xF_3

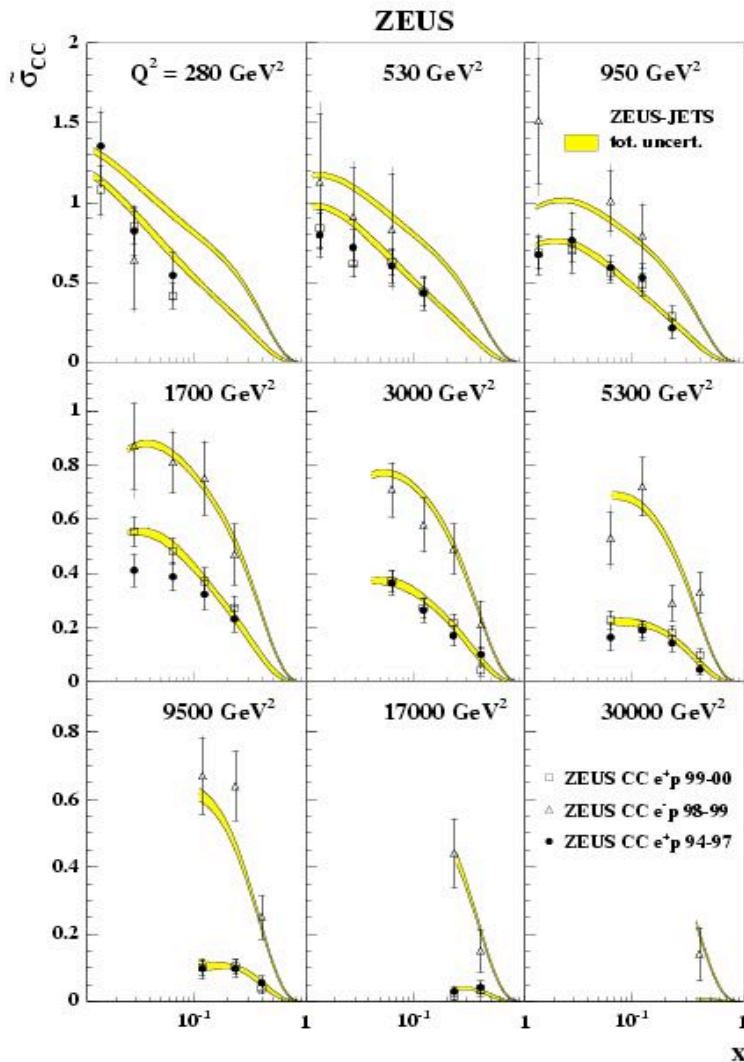
ZEUS



- Difference between e⁺p and e⁻p cross sections gives xF_3
- xF_3 comes from interference between gamma and Z⁰ exchange processes

$$xF_3 \propto \sum_q x(q - \bar{q})$$

Charged current cross sections



- Different for e^+p and e^-p

$$\sigma \propto [u + c + (1 - y)^2 (\bar{d} + \bar{s})]$$

- e^-p sensitive to $u(x, Q^2)$

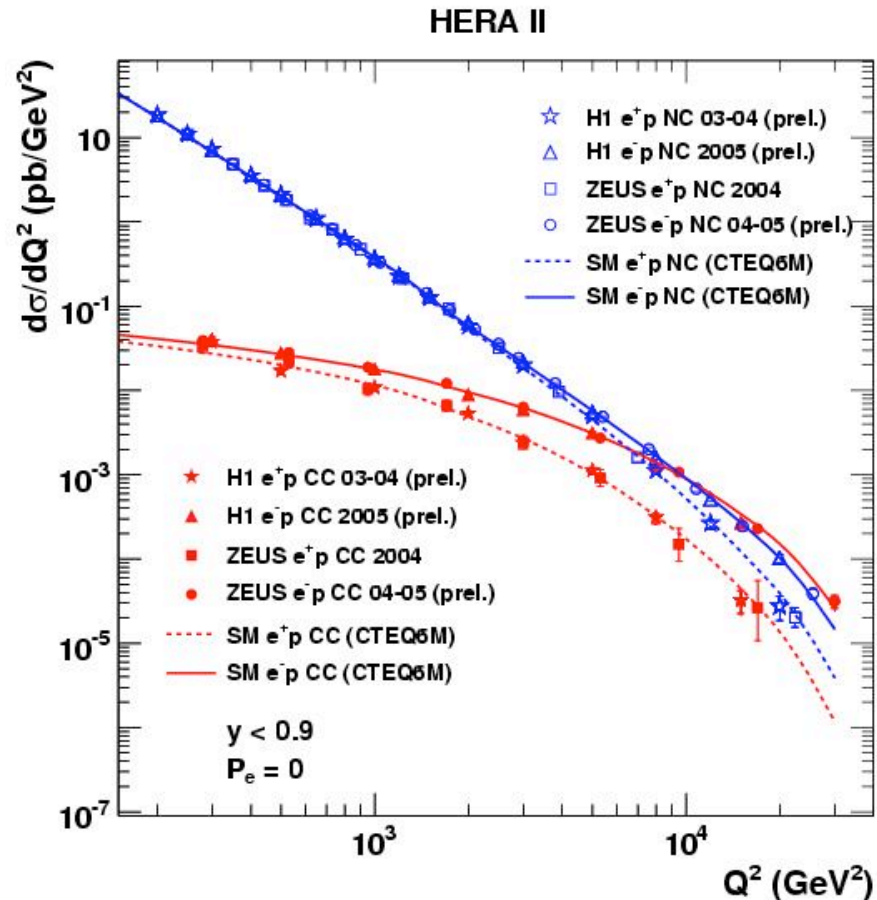
$$\sigma \propto [\bar{u} + \bar{c} + (1 - y)^2 (d + s)]$$

- e^+p sensitive to $d(x, Q^2)$
- e^+p suppressed by $(1-y)^2$ helicity factor

- Flavour specific probe of the proton
- e^+p data particularly valuable since $d(x, Q^2)$ poorly known

Electroweak unification at high Q^2

- Steep fall of NC cross section at low Q^2
 - $1/Q^4$ from photon exchange
- CC cross section suppressed by large mass of the W
 - $1/(Q^2+M_W^2)^2$
- Difference between e^-p and e^+p CC cross sections
 - $u(x,Q^2) > d(x,Q^2)$
 - e^+p $(1-y)^2$ helicity factor
- At high Q^2 ($Q^2 \sim M_W^2$) NC and CC same magnitude



Polarised DIS cross sections

NC cross section modified by P:

$$\frac{d^2\sigma(e^\pm p)}{dx dQ^2} = \frac{2\pi\alpha^2}{xQ^4} \left[H_0^\pm + PH_P^\pm \right] \quad P = \frac{N_R - N_L}{N_R + N_L}$$

Unpolarised contribution

Polarised contribution - only includes Z and γZ terms

Polarised contribution only significant at high Q^2 - subtle effect at HERA

CC cross section modified by P:

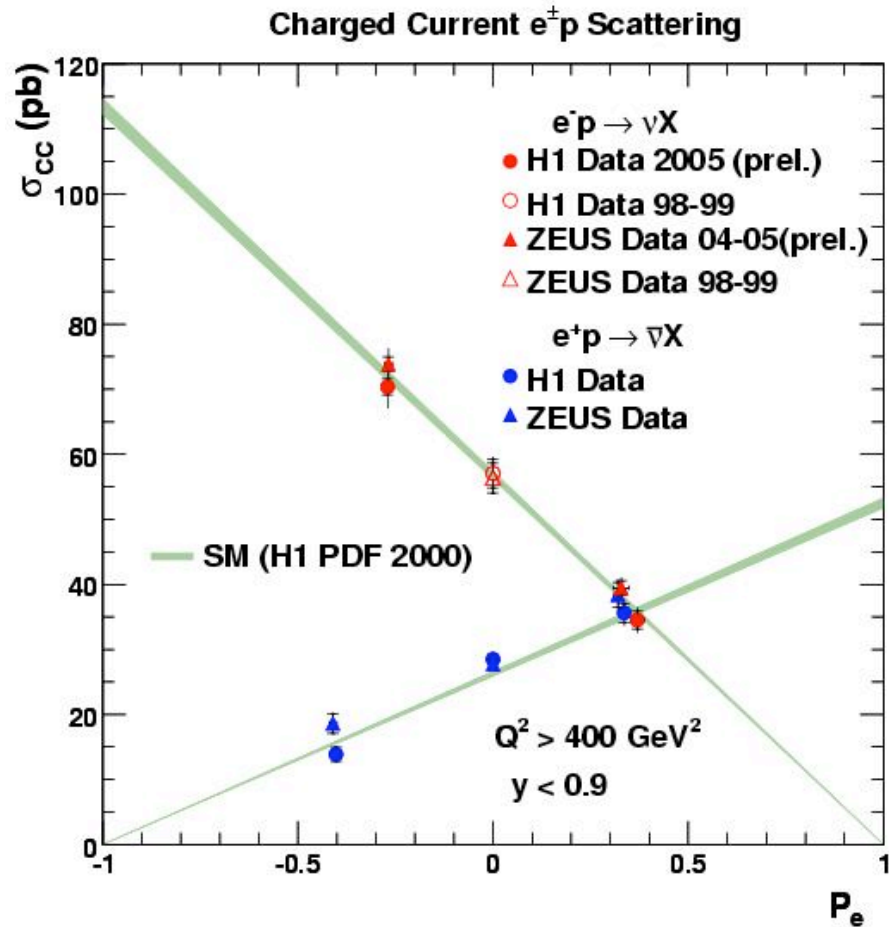
$$\sigma_{CC}^{e^\pm p}(P) = (1 \pm P) \cdot \sigma_{CC}^{e^\pm p}(0)$$

Polarisation scales P=0 cross section linearly - clear and large effect at HERA

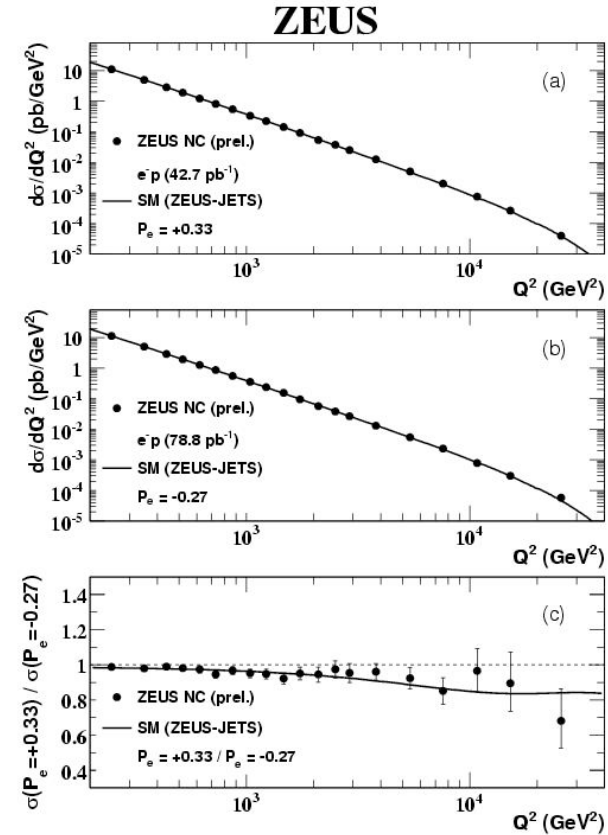
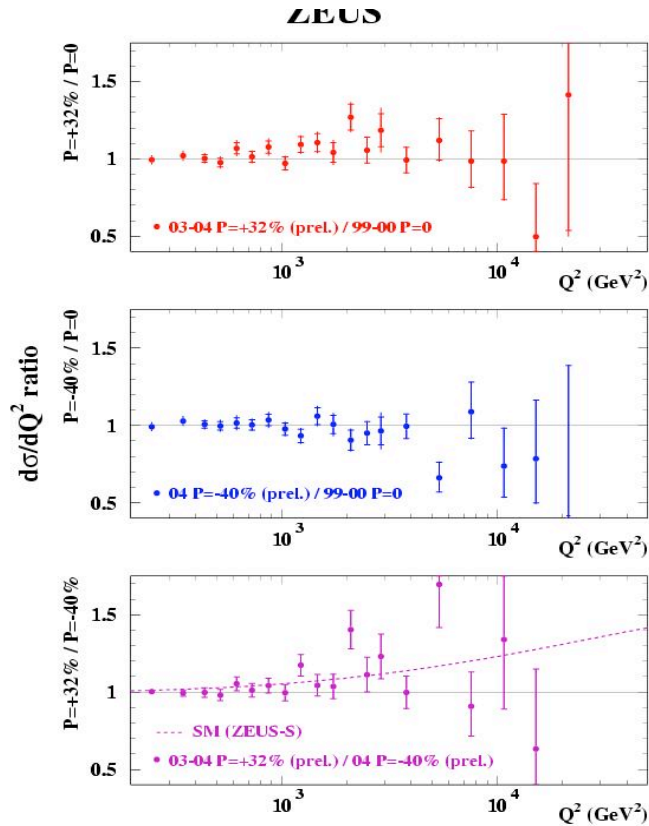
Pure V-A structure of the SM - no right-handed charged currents

Charged current cross sections

- First measurements of the polarisation dependence of CC DIS
- Cross section disappears as $P = -1(+1)$ for $e^+(e^-)p$
- Consistent with the chiral structure of the SM
 - Pure V-A interaction
 - No right-handed charged currents



Neutral current cross sections



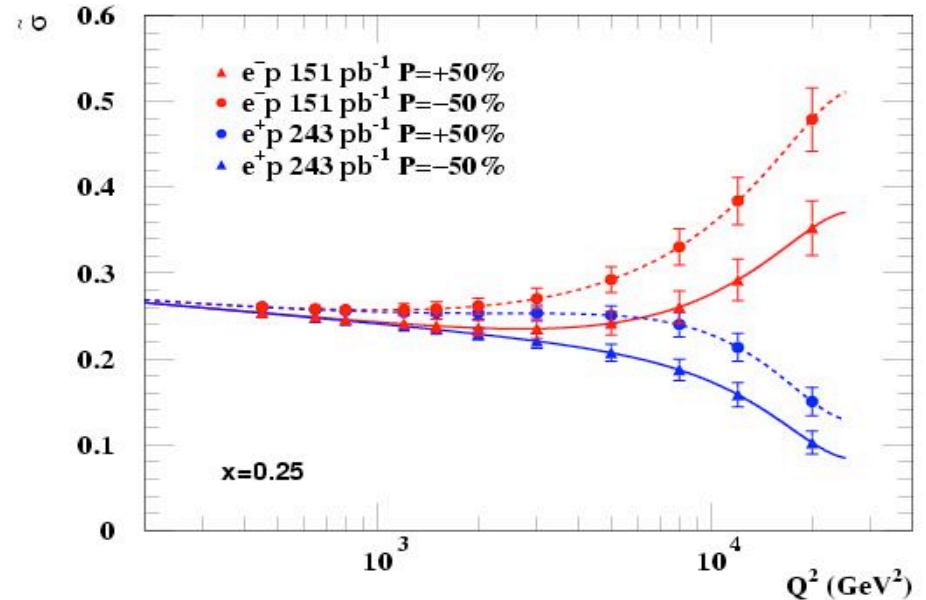
Polarisation effect more subtle in NC (only related to Z^0 exchange)
 → Just about experimentally established

Future prospects for polarised measurements

Measure left and right handed cross sections for e^+p and e^-p Scattering in NC and CC

Search for evidence of right-handed charged currents

Extract couplings of Z^0 to the light quarks with high precision



Challenging!

Need highest possible luminosity and polarisation

Using structure function data to determine the proton PDFs

- pQCD only predicts the Q^2 evolution of the PDFs, not the x dependence
- Ideally, find analytic parametrisations of the PDFs which are consistent with Q^2 dependence predicted by QCD
 - In practice, this is not possible
- Most common alternative method: perform direct numerical integration of the DGLAP equations at Next-to-leading-order (NLO)

Determining the proton PDFs

- The basic recipe for extracting PDFs:
 - Assume different analytic shapes for the PDFs (valence, sea & gluon) at some starting scale $Q^2 = Q_0^2$
 - Q_0^2 is arbitrary, but must be large enough for $\alpha_s(Q_0^2)$ to be small
 - Use the DGLAP equations to evolve the PDFs up to a different Q^2 value & use to predict structure functions
 - Fit prediction to the data
- The parameters needed are: those needed to specify the analytic shapes of the PDFs, Λ_{QCD} and $\alpha_s(M_Z^2)$
 - Can use these fits to determine α_s as well as the PDFs

Determining the proton PDFs

- A typical choice of PDFs to fit are:

$$u_v, d_v, S, g, \bar{d} - \bar{u}$$

- The usual form for the different PDFs are:

$$xu_v = A_u x^{\lambda_u} (1-x)^{\eta_u} P(x, u)$$

$$xd_v = A_d x^{\lambda_d} (1-x)^{\eta_d} P(x, d)$$

$$xS = A_S x^{-\lambda_s} (1-x)^{\eta_s} P(x, S)$$

$$xg = A_g x^{-\lambda_g} (1-x)^{\eta_g} P(x, g)$$

$P(x, i)$ are polynomials in x or \sqrt{x}

Not all normalisations A_i are free parameters: A_u , A_d & A_g are constrained by different sum rules

Contributions to the sea quark distribution

- Flavour composition of the sea
 - Heavy quarks require special treatment; assume either
 - Entirely generated by gluon distribution via $\gamma^*g \rightarrow qq$ ($Q^2 \sim m_{c,b}^2$)
 - Heavy quark distribution only above threshold ($Q^2 \gg m_{c,b}^2$)
 - Strange quarks suppressed wrt to u & d (larger mass)

$$\bar{s} = (\bar{u} + \bar{d}) / 4$$

- Historically assume u,d content of sea = symmetric
- No particular reason why this should be true !
- In fact, it appears that $\bar{d} > \bar{u}$

Where do different constraints come from ?

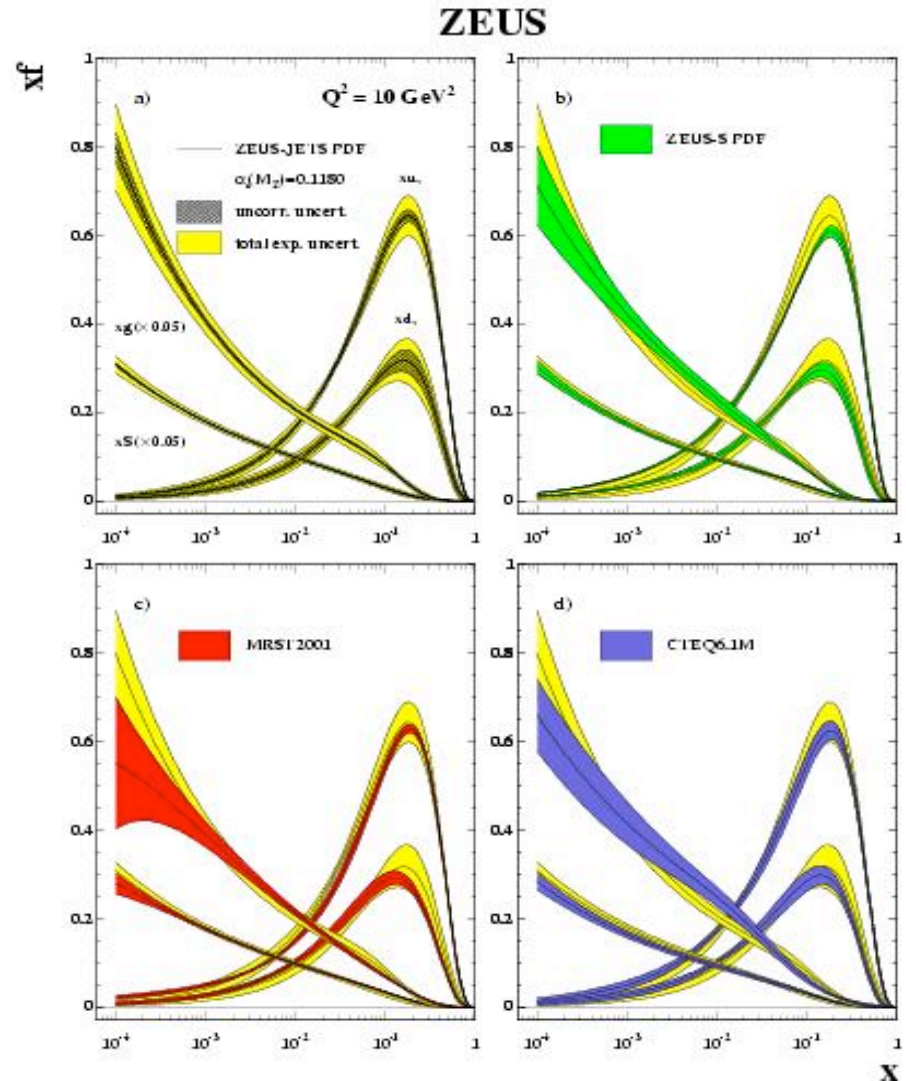
- CCFR neutrino data (xF_3)
 - Valence shapes for all x with u_v & d_v contributing equally
 - Most reliable at medium x (worry about nuclear corrections at highest and lowest x)
- NMC data on $F_2(\mu d)/F_2(\mu p)$
 - gives ratio d_v/u_v at large x
 - Only dataset to do so
- $F_2(D)$ & $F_2(lp)$ from NMC, BCDMS, E665, SLAC and F_2 from CCFR
 - Singlet combination of quarks ($x\Sigma = xu_v + xd_v + xS$)
 - Sea distribution for all (x, Q^2) covered by experiments

Where do different constraints come from ?

- F_2 data from same experiments
 - Combinations of u and d valence distributions at high x
 - Contributions weighted by (quark charge)² $\Rightarrow u_v$ distribution dominates for proton targets
 - Contribute equally for Deuterium targets
 - u_v better determined than d_v
- F_2 data also constrain gluon density
- CCFR dimuon data
 - Strange quark distribution
 - Directly or via weak decay of charm quarks
- HERA data: sea quark and gluon distributions

Results of QCD fits

- Results from different groups
MRST & CTEQ
“professional” fitters and
market leaders
- In these “global” fits other
data, aside from structure
function data, is also used
- What are these data ?



Information on PDFs from non-DIS processes

- Constraining quark distributions:
- Drell-Yan dilepton production: $pN \rightarrow \mu^+\mu^- X$
 - Considered sensitive probe of sea quark distribution
 - Dominant subprocess: $\bar{q}q \rightarrow \gamma^* \rightarrow \mu^+\mu^-$
 - Data from E605 and more recently E772 (moderate to high x)
- Ratio of data $pn \rightarrow \mu^+\mu^- X$ to $pp \rightarrow \mu^+\mu^- X$
 - Give information on ratio $\frac{d}{\bar{u}}$ (NA51 & E866 experiments)
- W^\pm production:

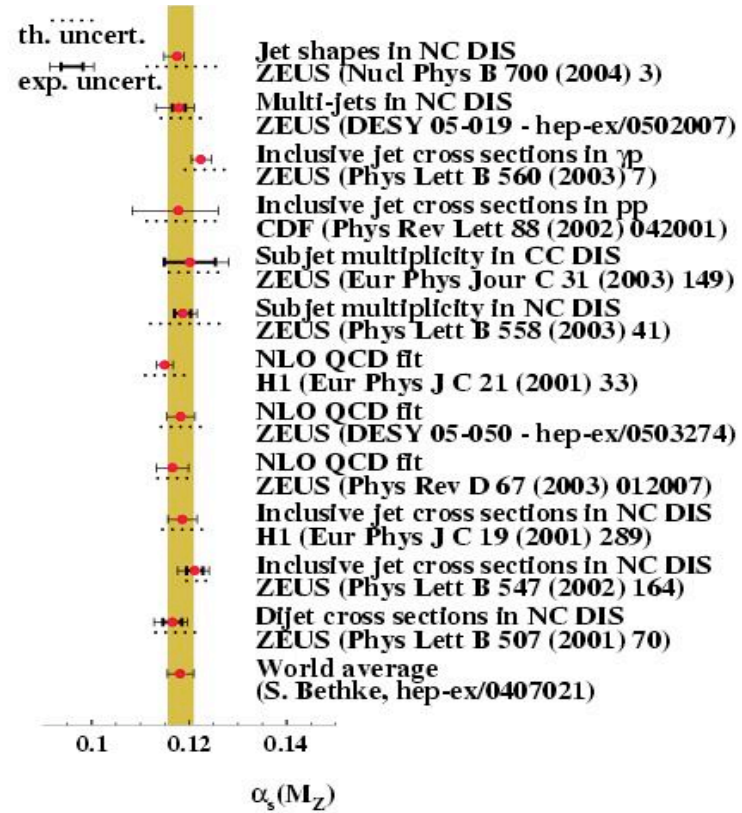
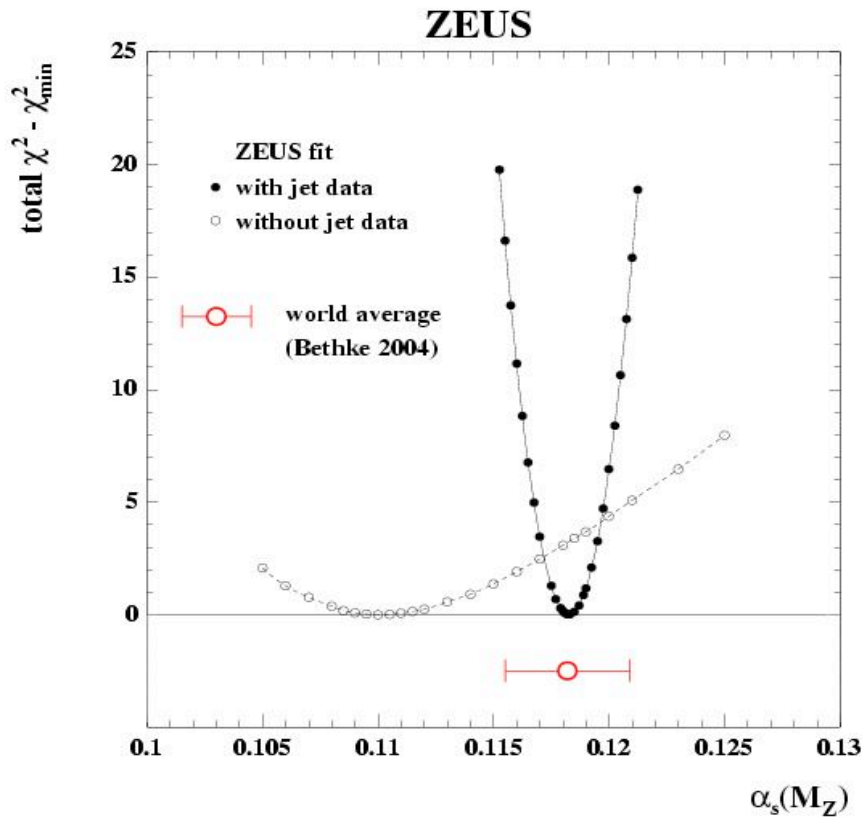
$$p\bar{p} \rightarrow W^+ (W^-) X$$

Dominant subprocesses: $u\bar{d} \rightarrow W^+, d\bar{u} \rightarrow W^-$

Information on PDFs from non-DIS processes

- The W^\pm charge asymmetry also gives information on d/u
- Constraints on the gluon distribution
 - DIS structure function data only really constrains low-x gluon
 - Use prompt photon or single inclusive jet production to get high-x gluon
- Prompt photon data: $pN \rightarrow \gamma X$ ($0.02 < x < 0.5$)
 - Dominant subprocess: $gg \rightarrow \gamma q$ at leading order
 - Data from WA70, UA6, E706, ISR, UA2 and CDF
- High E_T jet production from HERA and Tevatron
 - Depend on the gluon via gg , gq and $g\bar{q}$ initiated processes

α_s determination

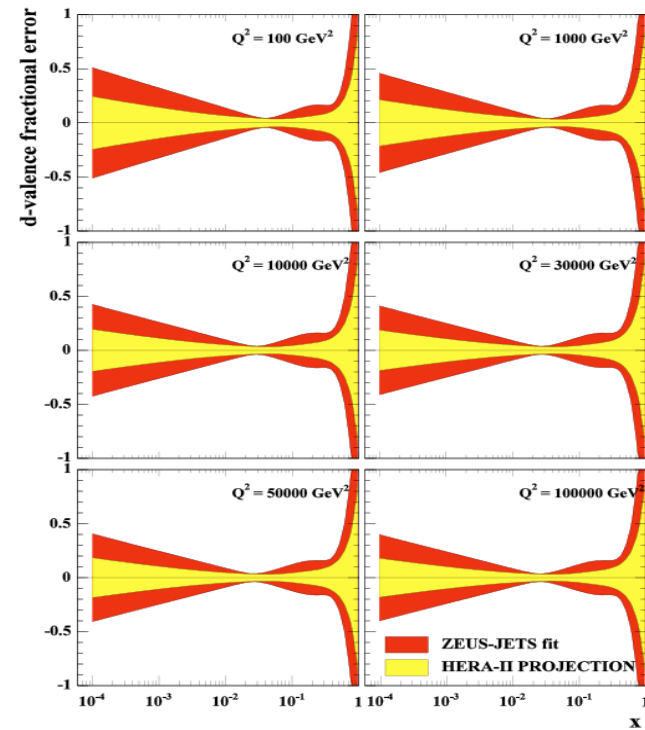
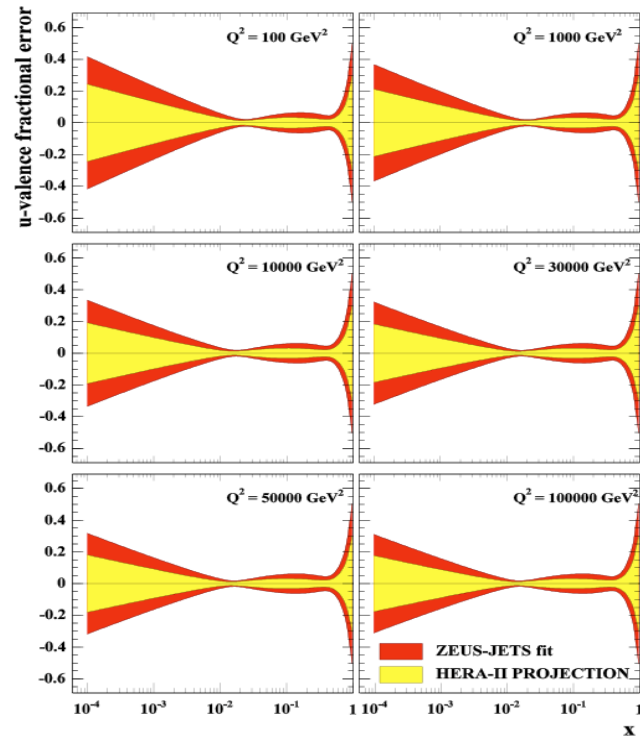


Jet data constrains α_s :

$$\alpha_s(M_Z) = 0.1183 \pm 0.0028 \text{ (exp)} \pm 0.0008 \text{ (model)}$$

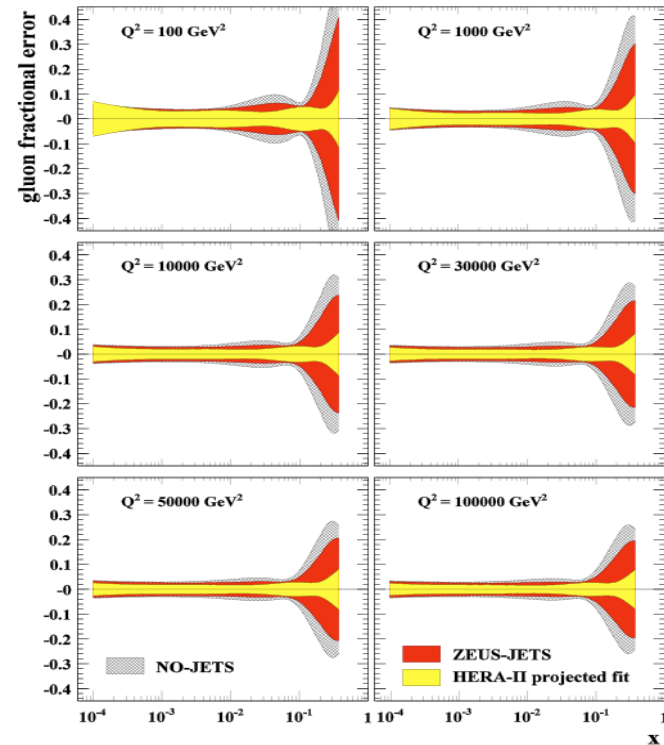
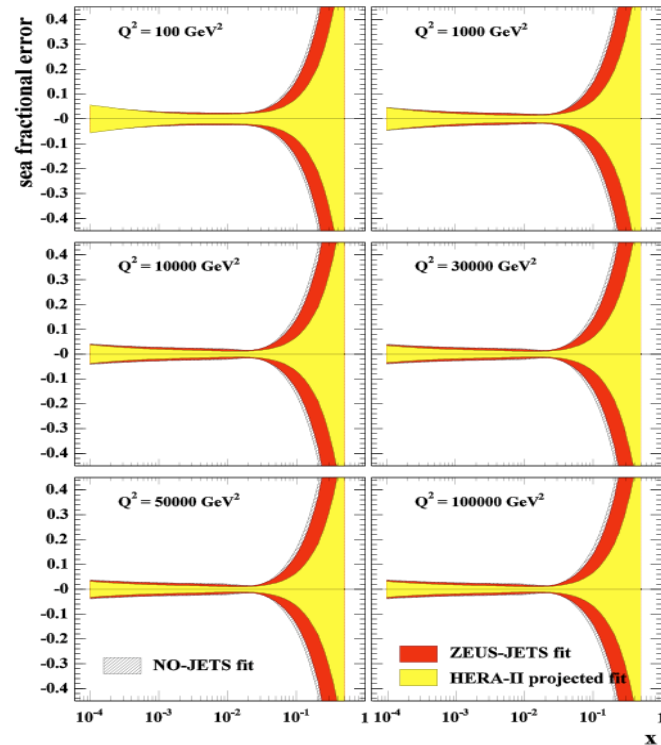
Theoretically limited! Need Next-to-Next-to-Leading-Order QCD

Future measurements



Valence quark distributions expected to improve in HERA II

Future measurements



Sea-quark and gluon distributions expected to improve in HERA II

→ Relevant for LHC processes

LHC applications

Example: W and Z production may be used for luminosity measurement at the LHC.

LO W and Z production

$$q + \bar{q} \rightarrow W / Z$$

x values given by

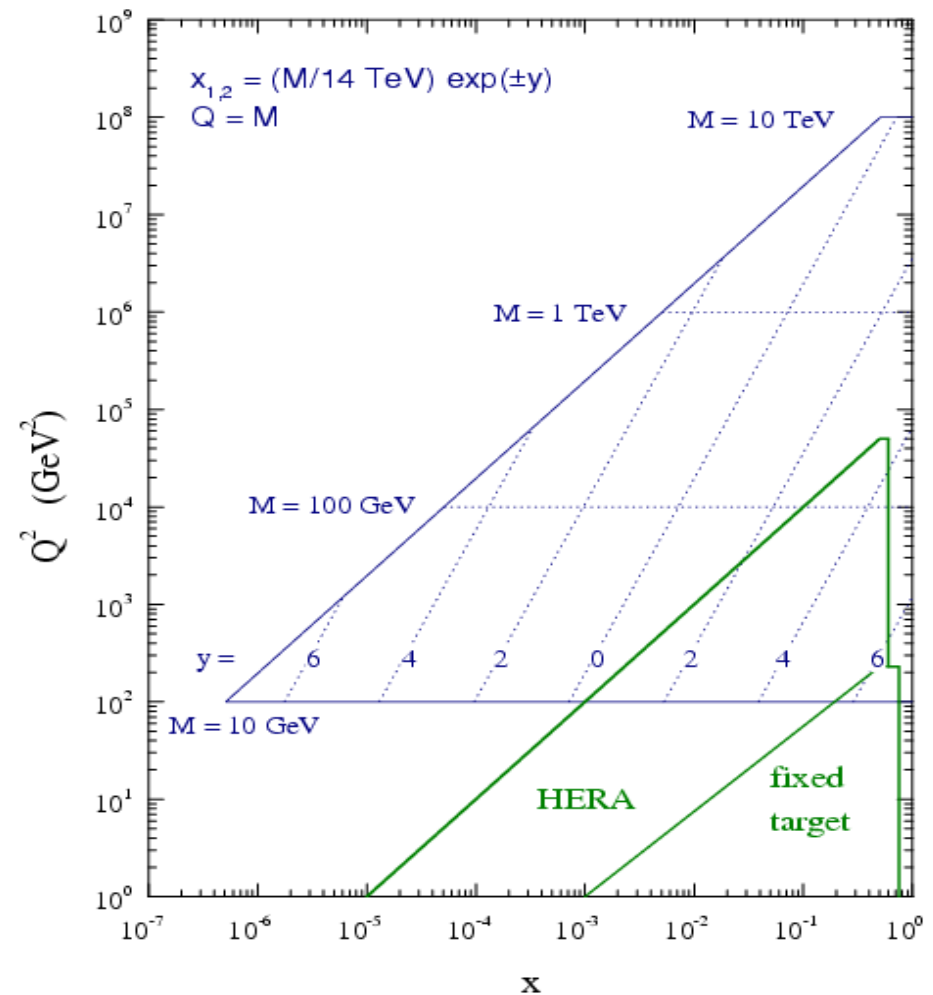
$$x_{1,2} = \frac{M}{\sqrt{s}} \exp(\pm y)$$

Central rapidity $x=0.005$

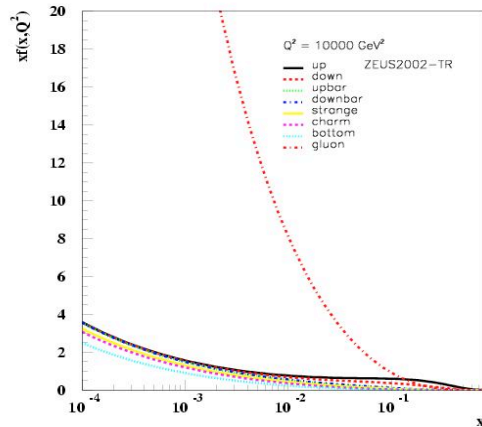
$$|y| < 2.5 \rightarrow 10^{-4} < x < 0.1$$

$$M \sim 100 \text{ GeV} \rightarrow Q^2 \sim 10000 \text{ GeV}^2$$

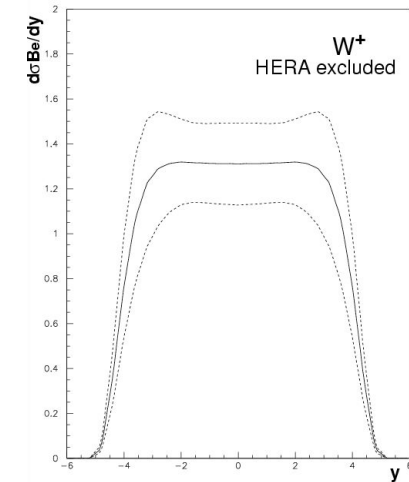
LHC parton kinematics



LHC applications

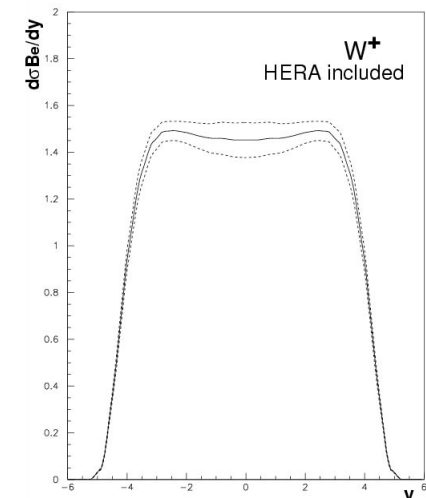


Pre HERA I



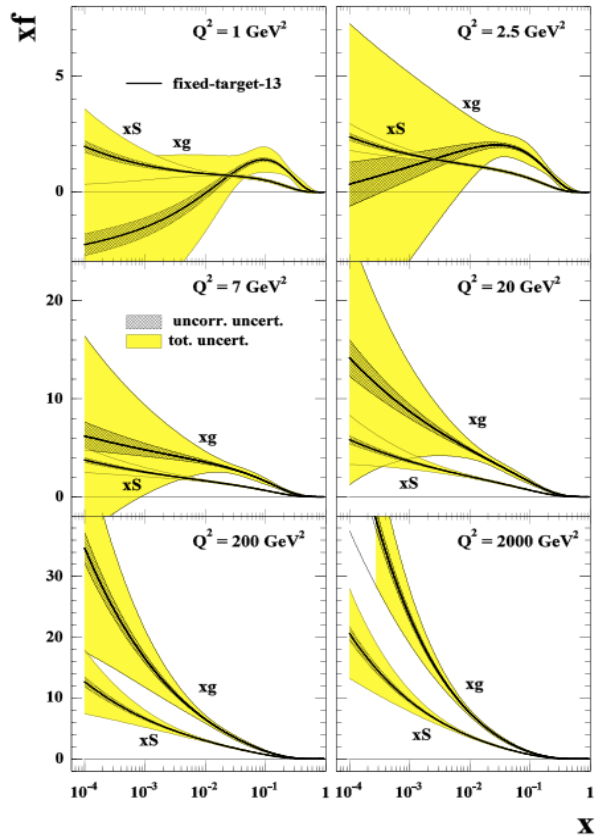
- Gluon PDF dominates at $Q^2=10000 \text{ GeV}^2$
- W and Z cross sections at the LHC depend crucially on the gluon distribution
- Before HERA large uncertainty in gluon and sea quark PDFs gave $\sim 16\%$ uncertainty
- Post HERA I uncertainty improves to $\sim 3.5\%$
- More improvement with HERA II
 - Probably good enough for LHC luminosity

Post HERA I

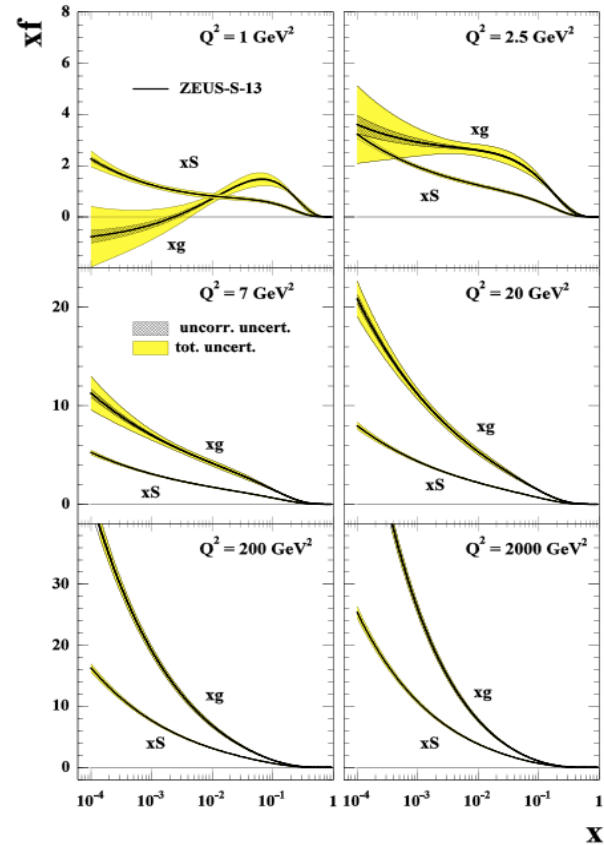


LHC applications

Pre HERA I

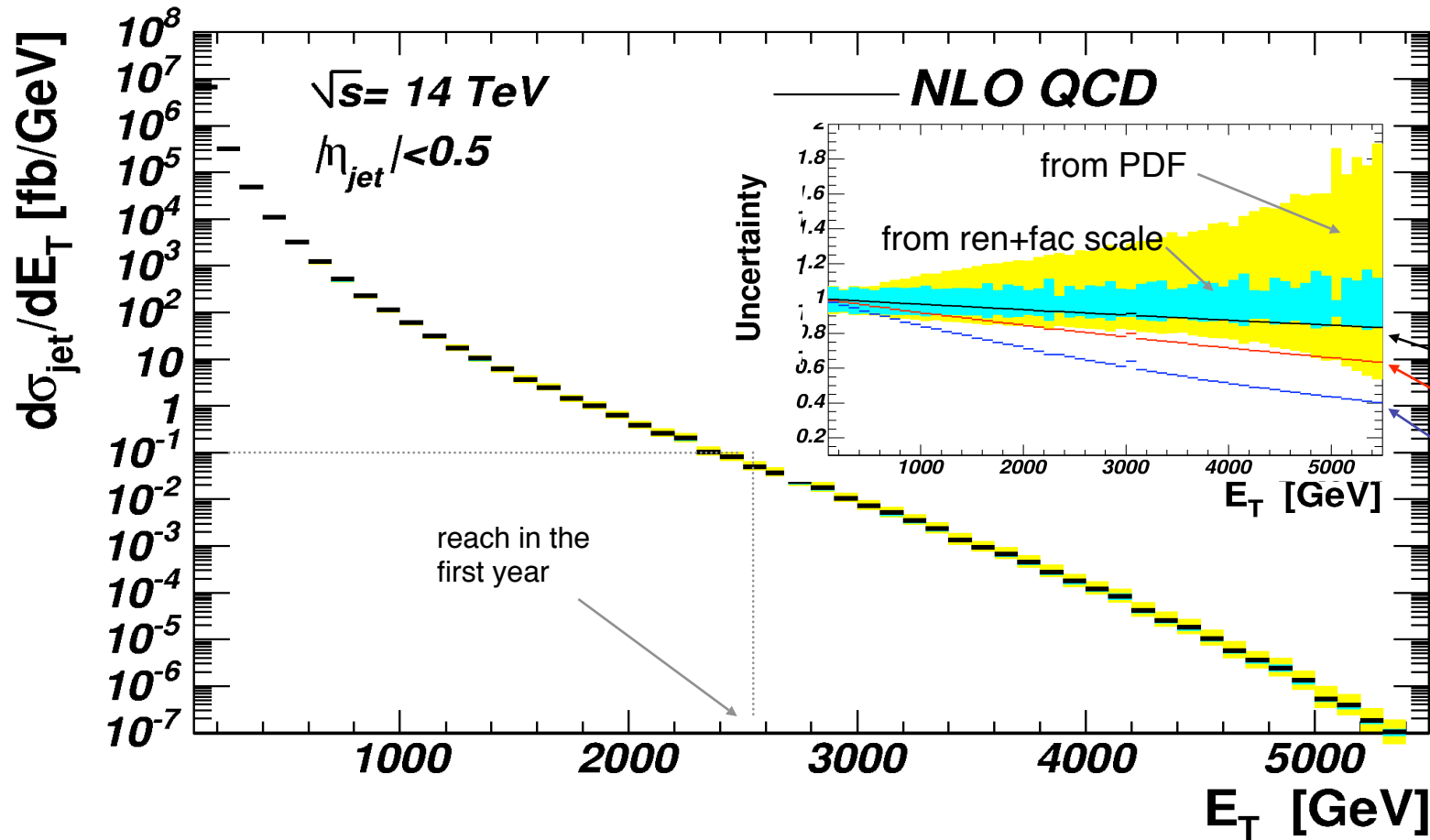


Post HERA I



Huge improvement in sea-quark and gluon uncertainties from HERA data

LHC applications



$$\sigma_{jet} = \sigma_{jet}^{SM} \cdot |A(\hat{s}, \hat{t})|^2$$

where

$$A(\hat{s}, \hat{t}) = e^{-\sqrt{f(\theta)\hat{s}}/M_s}$$

$M_s = 100 \text{ TeV}$

$M_s = 40 \text{ TeV}$

$M_s = 20 \text{ TeV}$

At very small distances, particles disappear into curled extra-dimensions

Example: String theory model (hep-ph/0111298)

Conclusion

- The ep and ed DIS experiments at SLAC in the late 1960's and the neutrino experiments of the early 1970's laid the foundations of QCD, the parton model of high energy interactions, and the entire language of modern particle physics.
- The high energy muon and neutrino scattering on nucleons and nuclei in the 1970's and 1980's expanded the kinematic range of DIS, and along with Drell-Yan and other hard scattering processes, allowed quantitative global QCD analyses of PDFs of the nucleons.
- The HERA experiments expanded the kinematic range into the small-x and high- Q^2 region by orders of magnitude, and pushed the accuracy to unprecedented levels.